An investigation of the mechanism of graphene toughening epoxy

Xiao Wang, Jie Jin and Mo Song*

Department of Materials, Loughborough University, Loughborough, Leicestershire, LE11 3TU, UK

ABSTRACT

The three different sized chemical functionalized graphene (GO) sheets, namely GO-1 (D_{50} = 10.79 μm), GO-2 (D_{50} =1.72 μm) and GO-3 (D_{50} = 0.70 μm), were used to fabricate a series of epoxy/GO nanocomposites. Fracture toughness of these materials was assessed. The results indicate that GO sheets were dramatically effective for improving the fracture toughness of the epoxy at a very significant low loading. The enhancement of the epoxy toughness was strongly dependent on the size of GO sheets incorporated. GO-3 with smaller sheet size gave the maximum reinforcement effect compared with GO-1 and GO-2. The incorporation of only 0.1 wt% GO-3 was observed to increase the fracture toughness of pristine epoxy by ~75 %. The toughening mechanism was well understood by fractography analysis of the tested samples. Massive cracks in the fracture surfaces of the epoxy/GO nanocomposites were observed. The GO sheets effectively disturbed and deflected the crack propagation due to its two dimensional structure. GO-3 sheets with smaller size were

* Corresponding author: Tel: +44 1509223160. E-mail address: m.song@lboro.ac.uk (M. Song)

highly effective in resisting crack propagation, and a large area of whitening zone was observed. The incorporation of GO also enhanced the stiffness and thermal stability of the epoxy.

---

1. Introduction

Toughening of thermosets has been a challenging issue that limits their applications in high performance areas such as automotive, aerospace and defence. [1] A high crosslinked density is always necessary for a thermoset material to achieve excellent mechanical properties. However, high crosslinked density could result in lower fracture resistance [1]. Traditional fillers such as rubber particles can improve the toughness of a thermoset resin. However, the micro fillers have seriously negative impact on manufacturability and mechanical properties of the final material [2]. It has been reported that with proper dispersion, nanofillers can effectively improve the toughness of thermoset materials [1].

Epoxy resins, which are the most important thermosetting resins in industry for various applications [3], have been reported to be successfully toughened by nanoparticles including metallic oxide (aluminium oxide and titanium oxide) [4], nano-silica [5,6], polyhedral oligomeric silsesquioxane [7], clay [8], carbon nanotubes [9,10] and graphene based nanoparticles [11-15]. Among these nanoparticles,

graphene is a new kind of carbon nanofillers with two-dimensional structure [16]. Its advantages in mechanical reinforcement over other carbon fillers such as expandable graphite, carbon black and carbon nanotubes were reported [11,17-19]. In the nano-toughening field, graphene based materials are superior to other non-two-dimensional fillers according to the Faber and Evans crack deflection modelling [20]. This theory predicts that for circular plate shaped particles with large aspect ratio, the tilting of the crack front acts as a very important toughening rule. It also suggests that neither the sphere nor the rod derive noticeable toughening from the crack tilting process. Accordingly, Rafiee et al. [11] compared the enhancement of toughness on epoxy by incorporation of various nanoparticles and concluded that graphene was the most effective one than other nanofillers. Qiu et al. [13] found that the incorporation of GO resulted in a different fracture morphology with coarser surface compared with neat epoxy. The presence of GO effectively prevented crack propagation by producing large amount of plastic deformation. Palmeri et al. [14] pointed that the presence of the coiled structure of graphene sheets could absorb significant amount of energy. Zhao et al. [21] studied the influence of the particle size of 2D nanofiller on improvement of epoxy toughness by computer simulation. The simulation results revealed that the stress concentration factor reduced as the particle size decreased, and when particle size was smaller than 1μm the stress concentration factor was unchanged. Very recently, Chatterjee et al. [22] reported that the bigger size of graphene sheets resulted in the greater reinforcement of fracture toughness for epoxy resin, which experimental result conflicts with Zhao's simulation result. So far,

although many studies on graphene toughening of epoxy resin have been made, some questions such as the one above mentioned still remain.

In our research, a series of epoxy/graphene oxide (GO) nanocomposites were successfully fabricated by addition of three different sizes of GO sheets. In this communication we attempt to evaluate whether the size of graphene sheet influences fracture toughness and also to develop an understanding of the toughening mechanism for the epoxy resin.

2. Experimental

2.1. Materials

Diglycidyl ether of bisphenol-A (DGEBA) epoxy (D.E.R*331) (epoxide equivalent weight is 182–192 $g{\cdot}eq^{-1}$) was provided by Dow Chemical. The 4,4'-Diaminodiphenylsulfone (DDS) curing agent was supplied by Sigma-Aldrich. Acetone was obtained from Fisher-Scientific Ltd. Three sizes of graphite flakes, which were denoted as G-1, G-2 and G-3, were purchased from Qing Dao Graphite Company (China). Their average size was 150 μm, 7 μm and 4 μm respectively.

.

2.2. Preparation of graphene oxide (GO)

GO powder was fabricated from graphite by Hummer's method [23]. The GO powder was denoted as GO-1, GO-2 and GO-3 according to different sizes of GO sheets.

2.3. Preparation of epoxy/GO nanocomposites

The dispersion of GO in acetone (1 mg·ml^{-1}) was achieved with ultrasonication for 30 min (300 w) at room temperature. DGEBA/GO mixtures were prepared by adding calculated amount of GO into DGEBA at elevated temperature, followed by stirring at 80 ^{o}C for 1 h. The mixtures were then placed in a vacuum oven for 12 h at 80 ^{o}C to remove the solvent. Calculated DDS curing agent (weight ratio of DDS/DGEBA = 1:4) was added in the DGEBA/GO mixture and stirred at 140 ^{o}C for 1 h. The mixture was poured into a mould and cured at 180 ^{o}C for 1 h, 200 ^{o}C for 2 h and post-cured at 250 ^{o}C for 2 h.

2.4. Characterisation of GO

The particle size distribution (PSD) of GO was measured by using a Malvern Instruments Mastersizer. The stirrer was set to be 900 rpm and the beam length was 2.40 mm. Transmission electron microscopy (TEM) analysis on the GO sizes was conducted using a JEOL 2100 FX instrument. A Philips Tecnai F20 high-resolution transmission electron microscopy (HRTEM) was used to observe the layered GO platelet structure. The accelerating voltage was 200 kV. The GO powder was dissolved in acetone, and then dropped on copper grid for TEM images. Fourier transform infrared (FTIR) spectra of the three types of GO was recorded from 4000 to 600 cm^{-1} using a Shimadzu FTIR-8400s spectrophotometer with a 2 cm^{-1} resolution over 64 scans.

2.5. Characterisation of epoxy/GO nanocomposites

X-ray diffraction (XRD) analysis was performed using a Bruker D8 diffractometer. The X-ray beam is Cu Kα, (λ=0.1542 nm) radiation operated at 40 kV and 40 mA. The X-ray diffraction patterns were scanned over a Bragg angle (2θ) from 1-30^{o} at a rate of 1^{o}/50 sec. TEM analysis was conducted to examine the thickness of agglomerated GO particles within epoxy matrix. The samples were cut into 50-nm-thin sections at room temperature, using a Huxley-Ultra Microtome cutting machine. Mode I fracture toughness (K_{Ic}) tests for pre-notched samples of epoxy and its composites were conducted on LR50K, Lloyd Instruments tensile testing machine by following ASTM standard D5045-99. The fracture toughness tests were conducted at room temperature with a crosshead speed of 1 mm·min^{-1} and a span width of 50 mm. For each sample, at least four specimens were tested. Tensile test was also carried out using the LR50K machine at a crosshead rate of 5 mm·min^{-1}, following ASTM D638 standard test method, at least five specimens were tested for each sample. The crack propagation was observed by using optical microscopy MEF-3. A field emission gun scanning electron microscopy (FEGSEM) LEO 1530VP instrument was used to observe the dispersion and fracture cross-sectional morphology of the nanocomposites. The dispersion images were taken from the non-whitening zone, where the number of cracks was minimal, in order to get a good observation of GO dispersion. TA instruments differential scanning calorimetry (DSC) 2920 calorimetry was used for the determination of the glass transition temperature (Tg) of epoxy nanocomposites. Nitrogen gas rate was set at 60 ml/min. All the

samples were heated from room temperature to 220 ^{o}C at a rate of 3 ^{o}C·min^{-1}. A modulated-temperature DSC model was used with modulation amplitude of 1 ^{o}C and a period of 60s. Three specimens were tested for each sample. Thermogravimetric analysis (TGA) was performed on a DSC-TGA 2950 instrument. The samples were heated from room temperature to 700 ^{o}C at a heating rate of 10 ^{o}C·min^{-1}. The rate of gas (air) was 50 ml·min^{-1}. In the swelling tests, Dimethylformamide (DMF) was chosen as the solvent. The tests were performed at 25^{o}C.

3. Results and discussion

Fig. 1 shows the particle size distribution of the three types of GO fillers. Obviously, the size decreases from GO-1 to GO-3. Table 1 lists the corresponding values of D_{20}, D_{50} and D_{80}. In particular, it can be noticed that the average size, D_{50}, of GO sheets for GO-1, GO-2 and GO-3 are 10.79 μm, 1.72 μm and 0.70 μm, respectively. Fig. 2 shows the TEM images of the exfoliated GO sheets prepared in acetone. The typical size of each GO can be observed. The GO sheets exhibits winkled surface texture. FTIR was also utilised to analyse the different sizes of GO sheets. FTIR spectra for GO-1, GO-2 and GO-3 are shown in Fig. 3, respectively. A very intense band between

2250 cm^{-1} and 2500 cm^{-1} was observed in the GO spectra, resulting from the presence of CO_2 in the testing atmosphere. The characteristic bands of GO were observed at 3420 cm^{-1} (-OH), 1745 cm^{-1} (C=O) and 1250 cm^{-1} (C-O-C), indicating that the graphene sheets were functionalized with hydroxyl, carboxyl (-COOH) and epoxide groups. Besides, =C-H and C=C bands were present in each GO spectrum, revealing the vibration of aromatic ring in graphene lattice. The peak position of =C-H band was located at 1400 cm^{-1} [24] for each GO spectrum, but the peak position of C=C is relative to the size of GO sheet. As summarized in Table 2, the peak position for GO-3 shifted to higher wavenumber compared to that of GO-1. This suggested that the conjugated effect of the graphene lattice became weaker as the size of GO sheet was smaller. Also, the content ratio of (=C-H)/(C=C) increased from GO-1 to GO-3, revealing the decrease in the lattice size. The FTIR analysis was in an agreement with the PSD and TEM results. On the other hand, the layered graphene platelet structure was studied by means of a HRTEM technique. Based on a sufficient quantity of observations upon the GO edges, for every type of GO sheets, they are composed of ≈ 2-5 individual graphene layers. Fig. 4 shows the typical layered structure for each GO category. The thickness of the GO sheets is about 1 nm. According to the PSD and HRTEM studies, the three GO varieties differ in their surface size but have similar thickness.

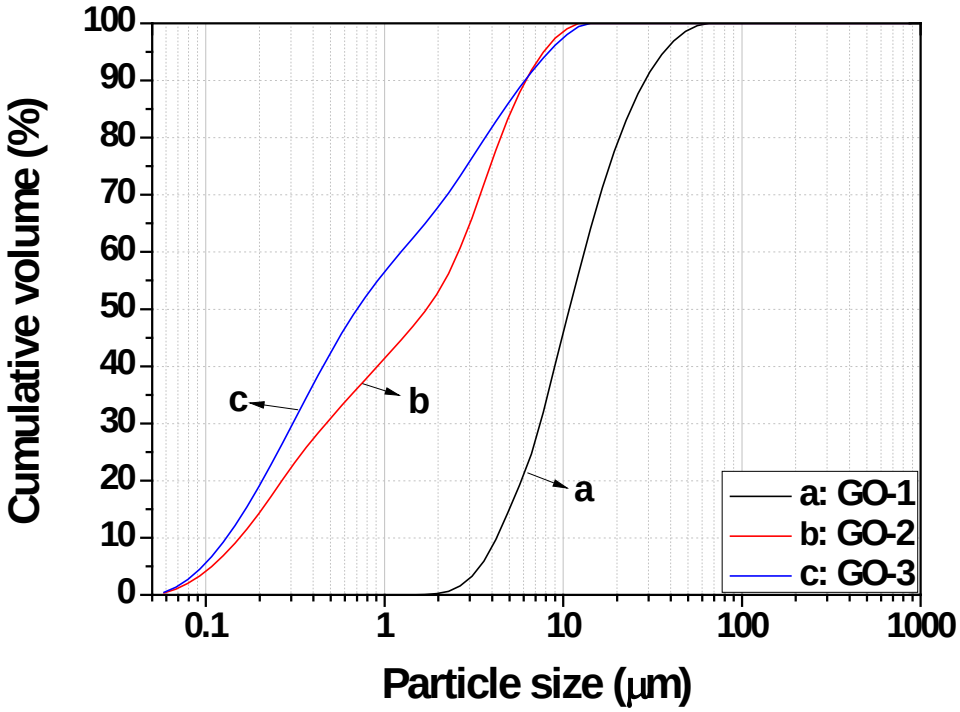

Fig. 1 – Cumulative volume versus particle size of (a) GO-1, (b) GO-2 and (c) GO-3.

Table 1 – Particle size distribution of GO.

Type	D_{20} (μm) [a]	D_{50} (μm) [a]	D_{80} (μm) [a]
GO-1	5.82	10.79	20.71
GO-2	0.27	1.72	4.48
GO-3	0.21	0.70	3.66

[a] D_{20}, D_{50} and D_{80} – particle sizes at which 20, 50 and 80 % of the sample is below this given size.

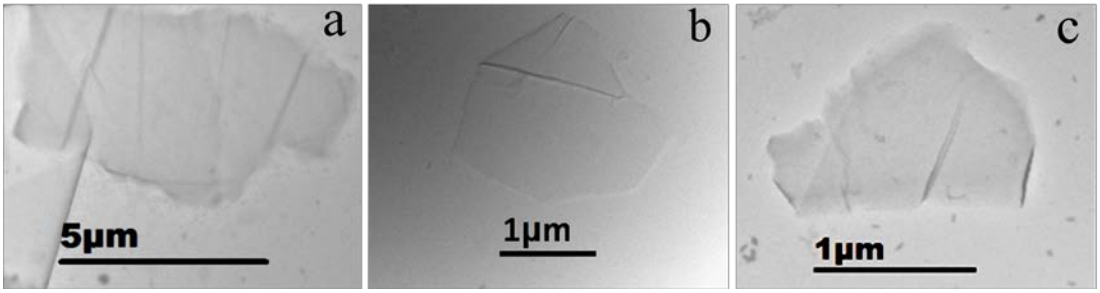

Fig. 2 - TEM images of (a) GO-1, (b) GO-2 and (c) GO-3 sheets, representing the typical size of each GO category.

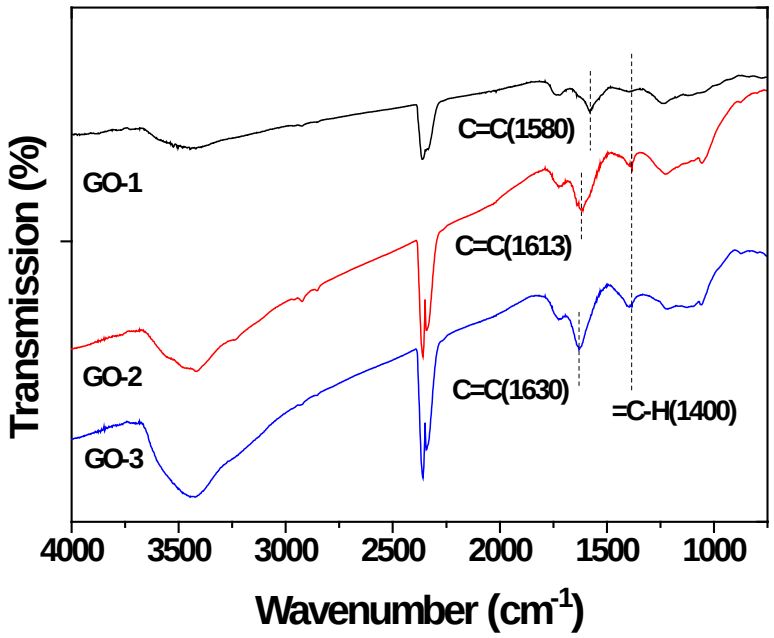

Fig. 3 - FTIR spectra of GO-1, GO-2 and GO-3. For clarification, the spectra were shifted parallel.

Table 2 - FTIR spectra analysis of GO lattice bands.

Lattice bands of GO	GO-1	GO-2	GO-3
Peak position of C=C /cm^{-1}	1580	1613	1630
Content ratio of (=C-H)/(C=C)	0.09	0.23	0.28

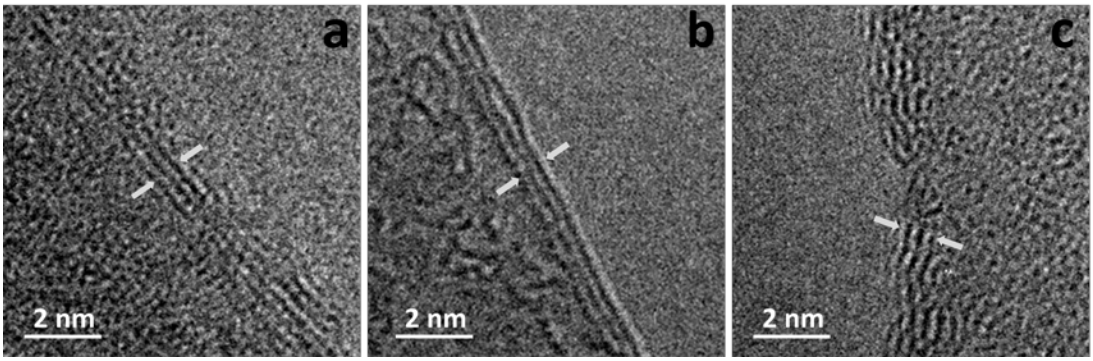

Fig. 4 – HRTEM images of the edges of typical graphene sheets for (a) GO-1, (b) GO-2 and (c) GO-3, showing the layered structure.

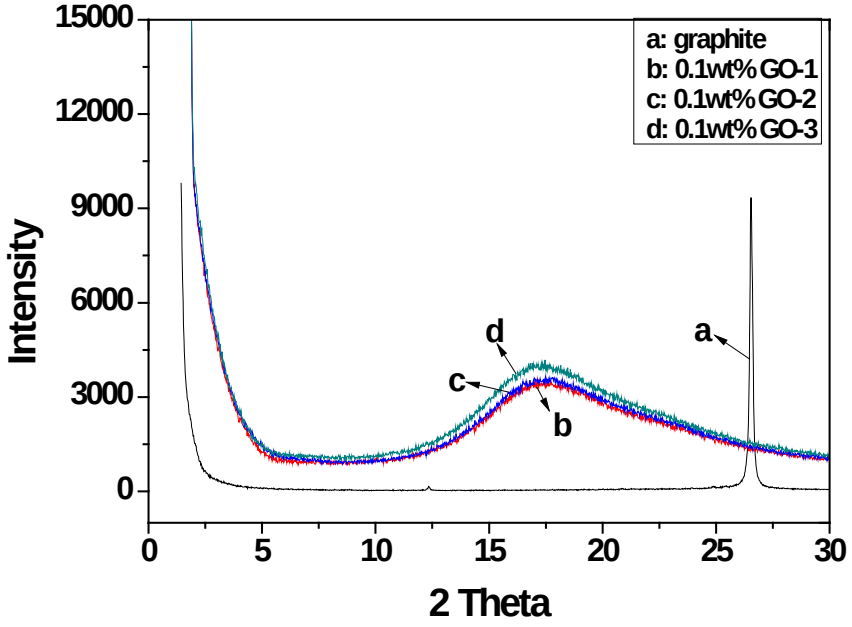

Fig. 5 - XRD patterns of (a) graphite and epoxy nanocomposites with 0.1 wt% (b) GO-1, (c) GO-2 and (d) GO-3.

Fig. 5 shows the XRD patterns of the graphite and epoxy/GO nanocomposites. The diffraction peak at about $2\theta=26^{o}$ corresponds to the (001) plane reflection of the graphite. The XRD results indicate that GO sheets in the polymer matrix did not show graphite-like ordered structure, proving the successful fabrication of the epoxy/GO

nanocomposites. GO-1, GO-2 and GO-3 showed similar exfoliation state in epoxy matrix. Moreover, the morphology of the GO sheets in matrix was observed via FEGSEM. The images of epoxy/GO nanocomposites with 0.1 wt% GO with different sizes were provided in Fig. 6 (a-f). Obviously, the GO sheets were well dispersed in the matrix, and the dispersion quality of the three types of GO was comparable. According to the PSD results, it can be found that the sizes of GO sheets were unchanged in the composites. Thus, the preparation process did not affect the original sizes of GO sheets. However, during the curing, particularly when the phase transition occurred, the nano-thick GO sheets had a great tendency to agglomerate to reduce configurational entropy. Their thickness could increase accordingly. Fig. 7 shows the TEM images of thin sections of the three epoxy nanocomposites with 0.1 wt% GO. It was observed that the thickness of the agglomerated GO sheets was ≈ 15-30 nm.

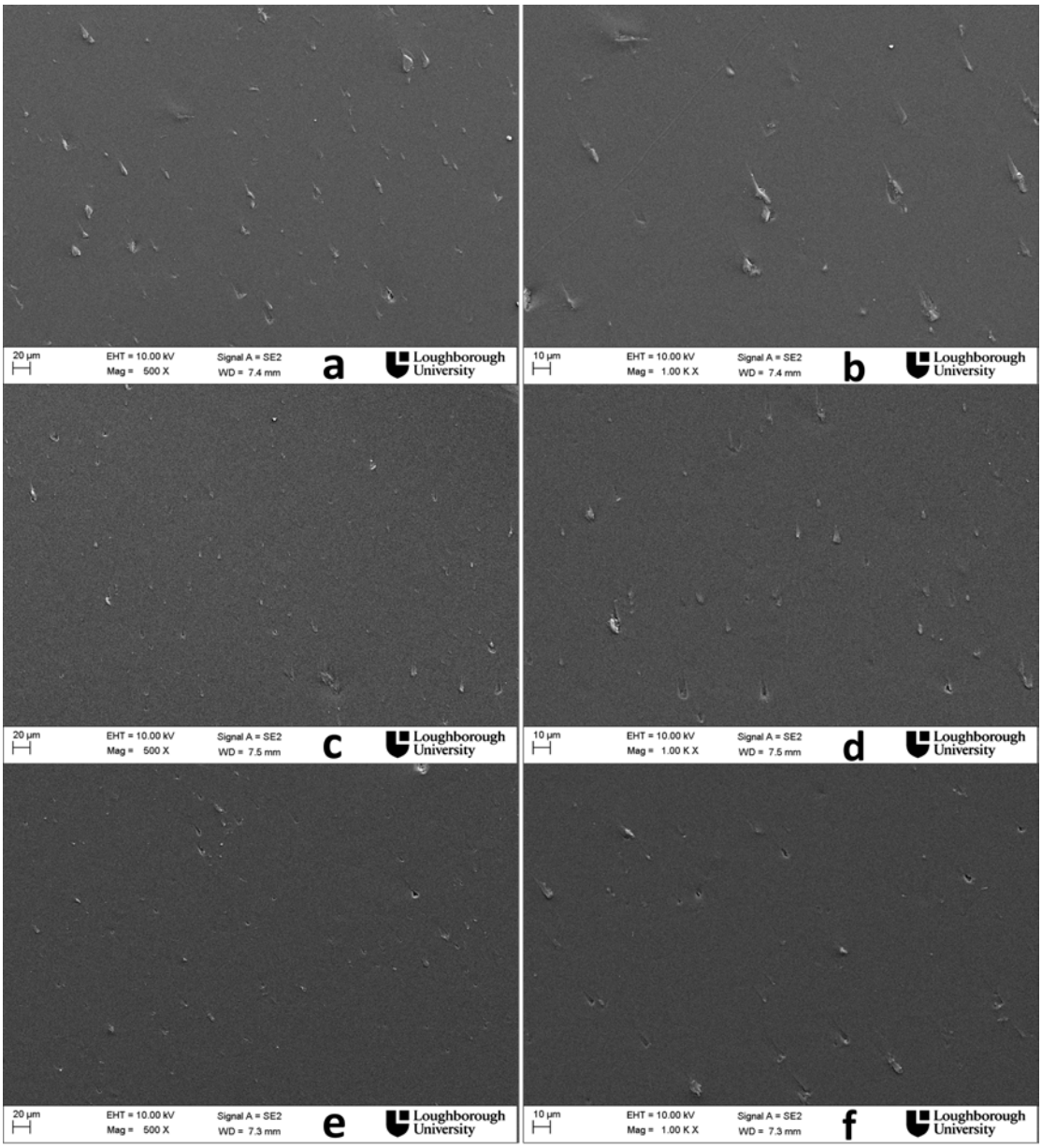

Fig. 6 - FEGSEM images of the dispersion morphology for epoxy/GO nanocomposites with 0.1 wt% (a, b) GO-1, (c, d) GO-2, (e, f) GO-3.

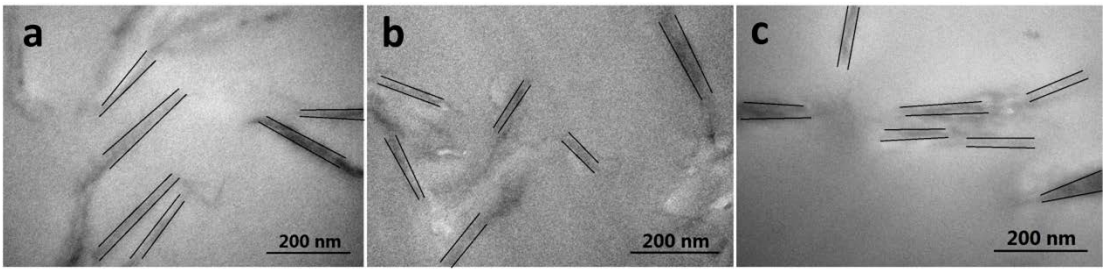

Fig. 7 - TEM images of epoxy nanocomposites with (a) GO-1 (b) GO-2 and (c) GO-3. The parallel lines show the thickness of agglomerated GO particles.

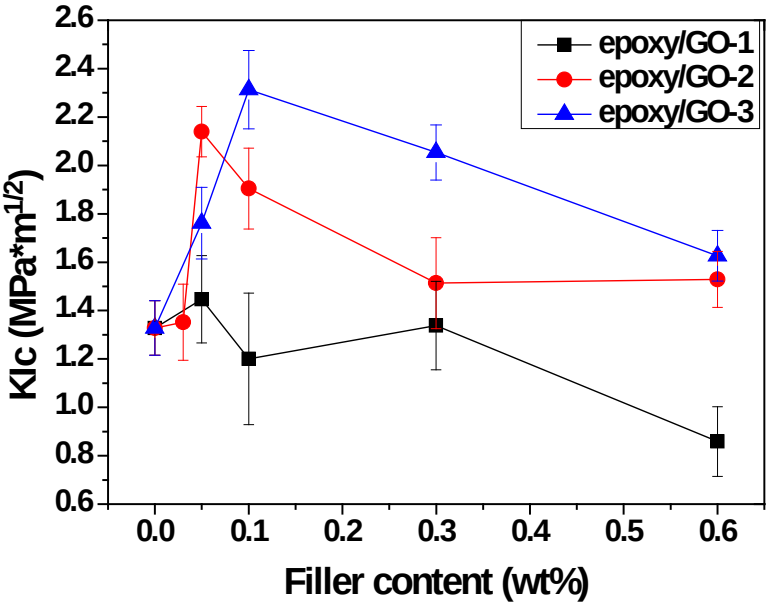

Fig. 8 - K_{Ic} versus GO content for the epoxy nanocomposites. The error bars represent standard deviations

Fracture toughness describes the ability of a material containing a crack to resist fracture and it is a critically important material property for design applications. Mode I fracture toughness (K_{Ic}) tests were applied to assess the toughness of the epoxy nanocomposites. The average values of critical stress intensity factor, K_{Ic}, are shown

in Fig. 8. The K_{Ic} value for the pure epoxy was about 1.32 MPa·$m^{1/2}$. Incorporation of GO-1 did not show obvious improvement of the fracture toughness for the pure epoxy. The property became even worse when higher GO-1 content was introduced. In comparison, the addition of GO-2 or GO-3 in the epoxy matrix caused a significant increase in fracture toughness with very lower loading. The K_{Ic} values for the GO-2 and GO-3 nanocomposite reached to 2.14 MPa·$m^{1/2}$ at 0.05 wt% GO-2 loading and 2.31 MPa·$m^{1/2}$ at 0.1 wt% GO-3 loading, respectively, which corresponds to a ~75 % increase in fracture toughness. For carbon nanotube epoxy composites, the best enhancement in K_{Ic} reported is ~43 %, which occurs at about fourfold higher nanofiller weight fraction [9]. In the case of nanoclay/epoxy composites it required about 3.5 % nanoclay weight fraction to achieve the similar level of K_{Ic} enhancement (~61 %) [25]. It was found that for higher loading fraction, the enhanced ability of GO sheets in K_{Ic} became weaker and finally begins to approach the pure epoxy value. The decrease of the fracture toughness enhancements could result from the degradation in the dispersion quality of GO at higher filler loadings [12]. The results indicate that the enhancement of fracture toughness were greatly dependent on the weight fraction and the size of the GO sheets. GO-3 with the sheet size of about 0.7 μm showed the best enhancement of the toughness and the 0.1 % weight fraction is an optimum concentration.

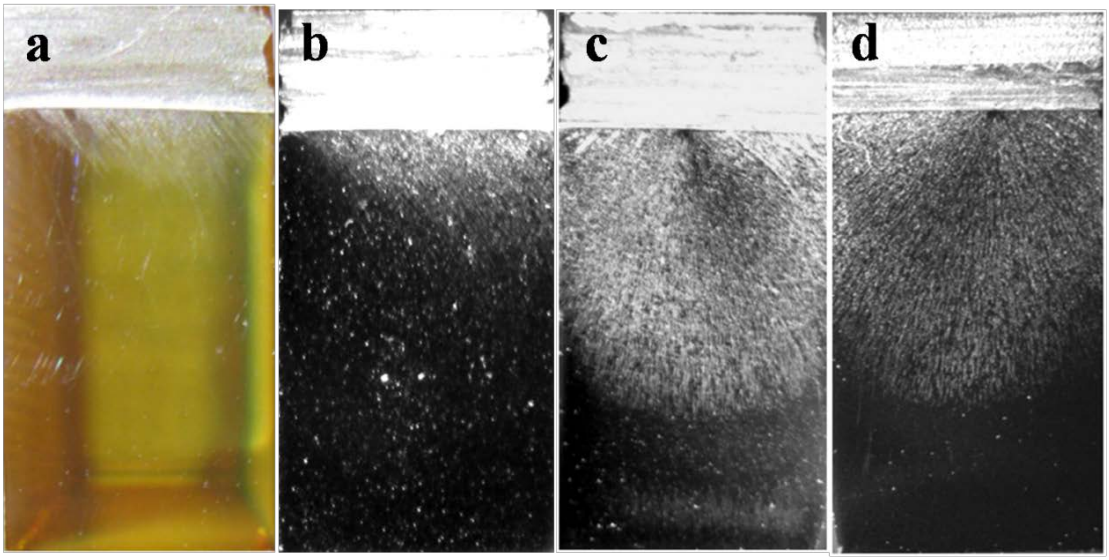

Fig. 9 - Digital images of the fracture surfaces for (a) the pure epoxy, and its nanocomposites with 0.1 wt% (b) GO-1, (c) GO-2, (d) GO-3.

Table 3 - Whitening zone percentage in the epoxy and its nanocomposites.

Sample	Whitening zone percentage
Epoxy	9 %
Epoxy/0.1wt% GO-1	13 %
Epoxy/0.1wt% GO-2	52 %
Epoxy/0.1wt% GO-3	54 %

A material's resistance to fracture crack propagation is important to prevent failure. According to brittle facture mechanism, the origin of the whitening zone is from the resistance of crack propagation; such information can identify fracture mechanisms for polymer nanocomposites. Fig. 9 shows the digital images of the fracture surfaces of the tested specimens for (**a**) the pure epoxy, and its nanocomposites with (**b**) 0.1 wt% GO-1, (**c**) 0.1 wt% GO-2, and (**d**) 0.1 wt% GO-3. A whitening zone was observed under the notched line for each specimen. A summary

of the percentage of the whitening zone area in the whole fracture surface is listed in Table 3. For the pure epoxy resin, the whitening zone area was only about 9 % observed under the pre-notched line. By addition of 0.1 wt% GO-1, the percentage of the whitening zone area slightly increased to 13 %. Remarkably, the percentage of the whitening zone area for the GO-2 or GO-3 based nanocomposites substantially increased to over 50 %. The results illustrate that the resistance to fracture crack growth dramatically improved by the presence of GO sheets in the epoxy matrix. The size-increased whitening zone is able to consume more energy when fracture occurs, corresponding to higher fracture toughness. The toughness of nanocomposites increased as the decrease of GO sheet size. It can be explained by Zhao's [21] simulation result, with regard to stress concentration factor. In their modelling for enhancing epoxy resin by 2D fillers at a fixed fraction, the stress concentration of composite was reduced as the decrease of particle size. Hence, GO-1 brought about high stress concentration in epoxy matrix, compared with GO-2 and GO-3. This could be the main reason for the disappearance of the fracture toughness enhancement for epoxy/GO-1 nanocomposites. Moreover, the graphene surface exhibits wrinkle-like texture [11, 19, 26]. The wrinkled texture changes the roughness and mechanical properties of graphene sheets. Uneven distributions of local spring constant and forces were observed in the stacks of graphene [27]. They could affect load transfer efficiency and stress distribution around the fillers. Wang et al. [28] indicate that, for a given edge contraction (ϵ) on a suspended graphene sheet, the wavelength (λ) and

amplitude (A) of the wrinkles and the out-of-plane displacement increased with the graphene size (L), according to Eq. (1).

$$\lambda^4 \approx 4\pi^2 \upsilon L^2 t^2 / [3(1 - \upsilon^2)\epsilon] \quad (1a)$$

$$A^4 \approx 16\upsilon L^2 t^2 \epsilon / [3\pi^2(1 - \upsilon^2)] \quad (1b)$$

Where t is the thickness and υ is the Poisson's ratio of graphene. In our study, all the GO varieties had similar thickness, Poisson's ratio and edge contraction, duo to the same preparation method and processing conditions. Although the interfacial bonding between GO and epoxy matrix could affect the state of graphene, the effect could be similar due to the similar Tg variation (see Fig 12 and its discussion) in the three systems. We believe that the bigger GO-1 sheets could possess large size wrinkles. The roughness was substantially increased. Also, the wrinkles were the main source that could pose the bending, twisting and folding of the graphene sheets [29]. The wrinkles and the deformation sites, which could be regarded as induced defects, were kept permanently in the composites after curing process. The regularity and geometric continuity were significantly reduced. Therefore, the presence of the size-increased defects reduced the load transfer efficiency in GO-1 sheets, and brought about serious local stress concentrations in regions surrounding the defects. It is believed that bigger size defect would result in stress concentration of composites in a larger area. According to brittle failure mechanism, the fracture stress is inversely related to the length of defects [30]. Hence, GO-3 that had smaller size of the induced defects, exhibited better reinforcement in epoxy toughening.

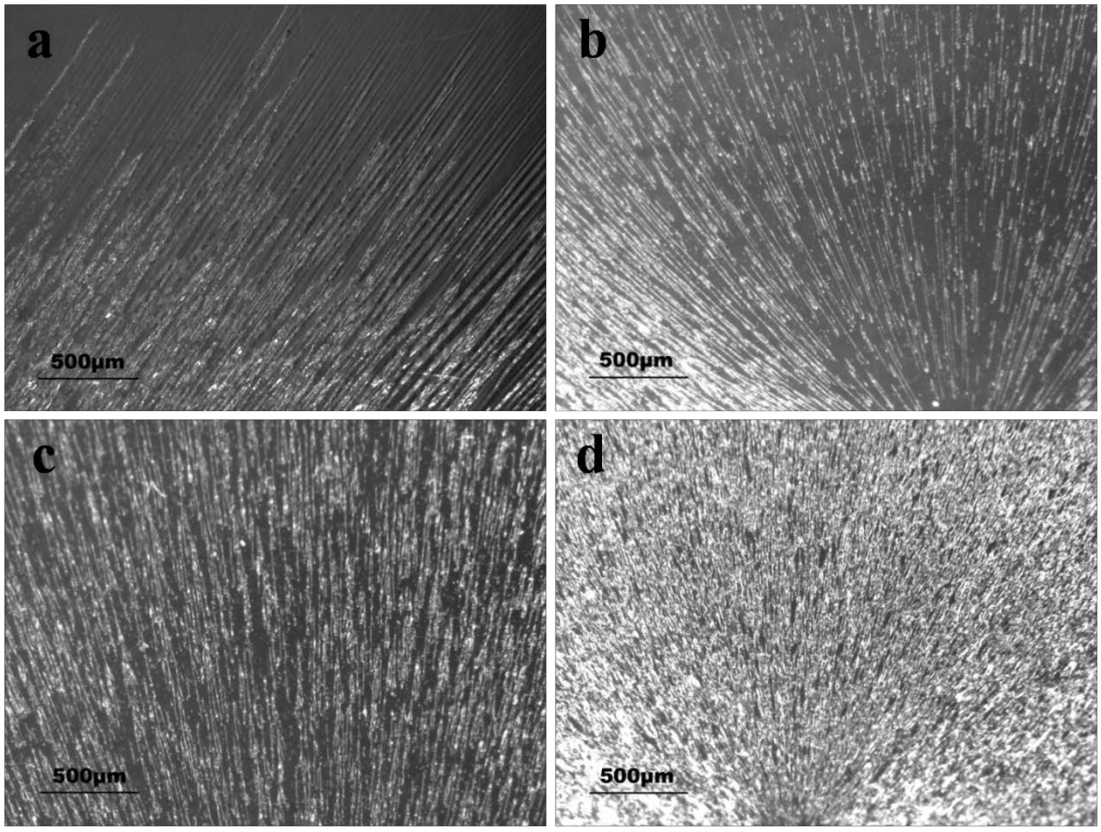

Fig. 10 - Optical microscopy images of crack propagation on the fracture surfaces (whitening zone) for (a) the pure epoxy, and its nanocomposites with (b) 0.05 wt% GO-3, (c) 0.1 wt% GO-3, (d) 0.3 wt% GO-3.

The fracture surfaces were further observed by optical microscopy (OM). The OM fractography for the pure epoxy and its GO-3 nanocomposites with different GO-3 contents are depicted in Fig. 10. It can be seen that a clear image of cracks which grow in the direction of crack propagation for the pure epoxy. By addition of GO sheets the development of cracks was effectively disturbed. In particular, the number of the cracks increased, but the average size of the cracks reduced as the GO content increased. Meanwhile, many sub-cracks were induced in the fracture surface of the nanocomposites. The crack propagation from the pre-notched line was deflected,

tilted or suppressed due to the presence of two-dimensional structured graphene sheets. The breakdown of propagating cracks certainly reduce local applied stress, thus contribute to the resistance of fracture [20]. Accordingly, this is one of the main reasons for the improvement of the fracture toughness. However, addition of significantly higher content of GO sheets led to induce massive sub-cracks or micro-cracks as shown in Fig. 10d, which could encounter more flaws during crack propagates in the nanocomposite. Stress concentration on the weakest flaw may result in the fracture of the nanocomposite [21]. The most effective enhancement of toughness for the epoxy resin was achieved at 0.1 wt% GO-3 loading.

The toughening mechanism can be further understood by SEM fractography analysis. As shown in Fig. 11, it was noticed that the pure epoxy resin exhibited typical brittle fracture surface and shows an oriented bamboo-like fracture patterns initialized from the cracks. The area between the bamboo-like patterns was very smooth, indicating the rapid crack propagating [31]. In contrast, GO/epoxy nanocomposites showed quite different fracture morphology. The bamboo-like fracture patterns was disturbed and gradually disappeared with increasing GO content. The surface appeared coarser and ditches with characteristic parabolic feature from crazes intersecting the main feature plane, indicating a crack deflection process occurred, where an initial crack tilts and twists when it encountered a rigid inclusion. This generates an increase in the total fracture surface area resulting in greater energy absorption as compared to the pure epoxy. SEM fractography analysis again evidenced that the GO resulted an increase of the toughness of the epoxy by

effectively preventing crack propagation.

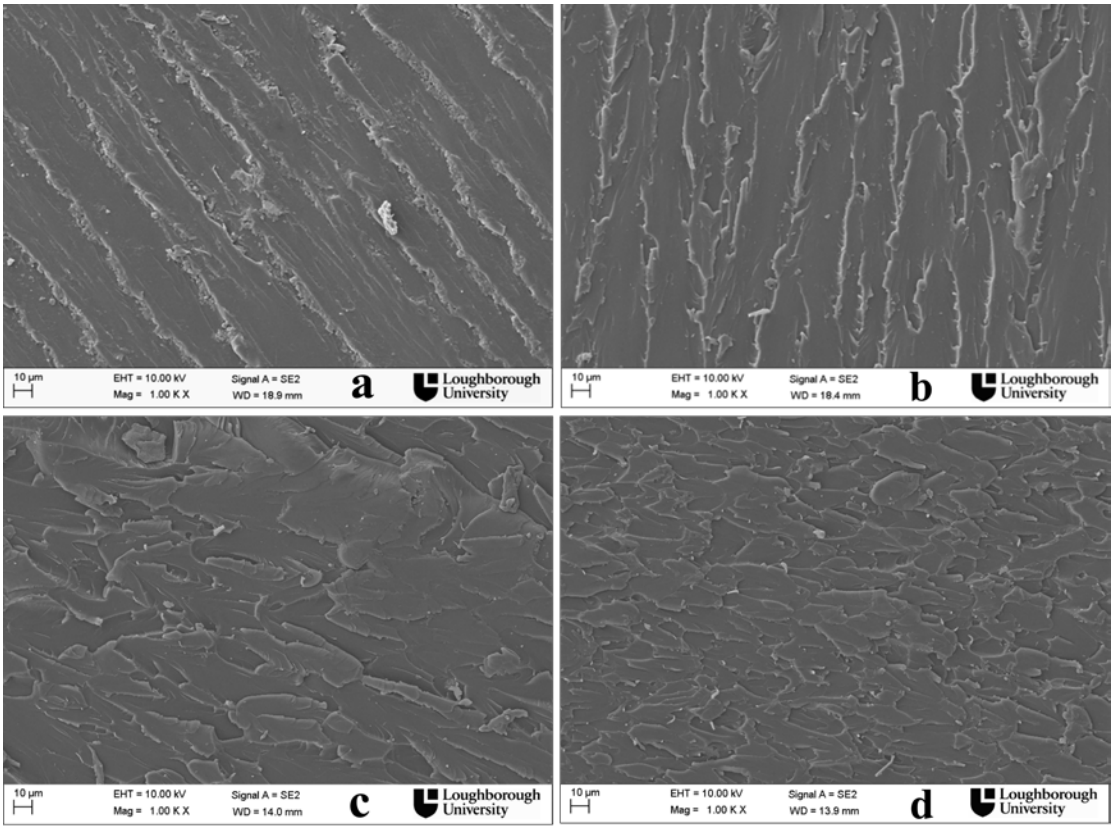

Fig. 11 - FEGSEM images of the fractured surface in the whitening zone for (a) the pure epoxy, and its nanocomposites with (b) 0.05 wt% GO-3, (c) 0.1 wt% GO-3, (d) 0.3 wt% GO-3.

From above discussion, the incorporation of GO-3 gave the maximum improvement in the toughness of epoxy resin, compared with GO-1 and GO-2. The mechanical and thermal properties for the epoxy/GO nanocomposites were also assessed. Fig. 12 shows the glass transition temperature of pure epoxy and its nanocomposites. It can be observed that the Tg increased as the increasing GO content. This could result from the enhanced interfacial bonding between epoxy

monomers and functional groups on graphene fillers [12, 19]. The crosslink density could slightly increase in the areas close to the fillers. Thus, the GO layers confined the interfacial epoxy chains by restricting their movement. Incorporation of 0.6 wt% GO led to an increase of ~ 11^{o}C, compared to the pure resin. Moreover, there was no difference in the Tg between the three types of nanocomposites. It is believed that the interfacial bonding could be similar in the three systems. The Young's modulus of the epoxy/GO nanocomposites were characterized and shown in Fig. 13. The addition of GO slightly increased the stiffness of epoxy resin. The reinforcement effect was from the transfer of the mechanical properties of the graphene, which was also attributed to the improved interfacial adhesion. The three GO showed similar improvement in the Young's modulus of epoxy. In contrast, the toughening mechanism indicates the importance of the two dimensional structure of GO that effectively resisted the crack propagation. Despite the three GO varieties showed comparable interfacial adhesion and dispersion within epoxy, the enhancement on the toughness differed significantly. We believe that Stress concentration factor, which related to the size of graphene, was critical in toughness improvement.

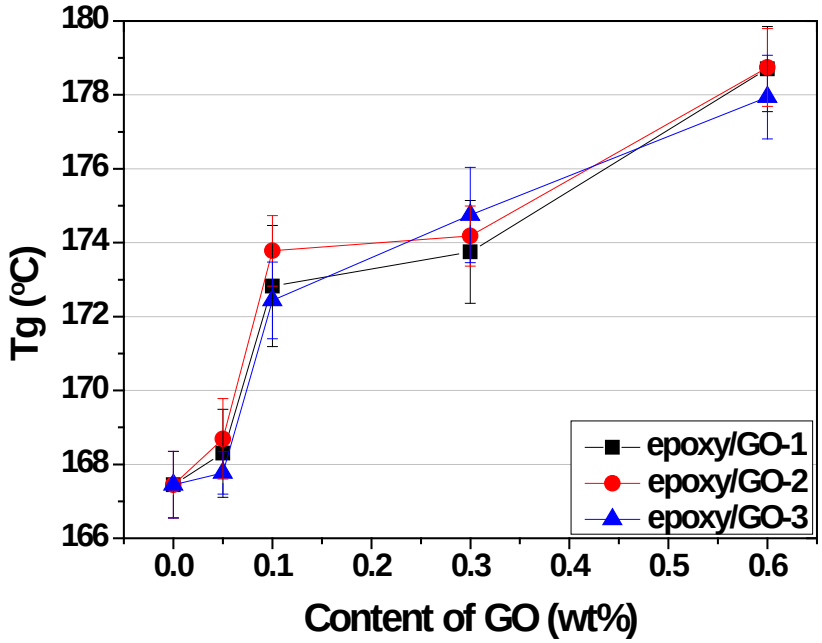

Fig. 12 - Glass transition temperature of epoxy and its nanocomposites with GO-3. The error bars represent standard deviations.

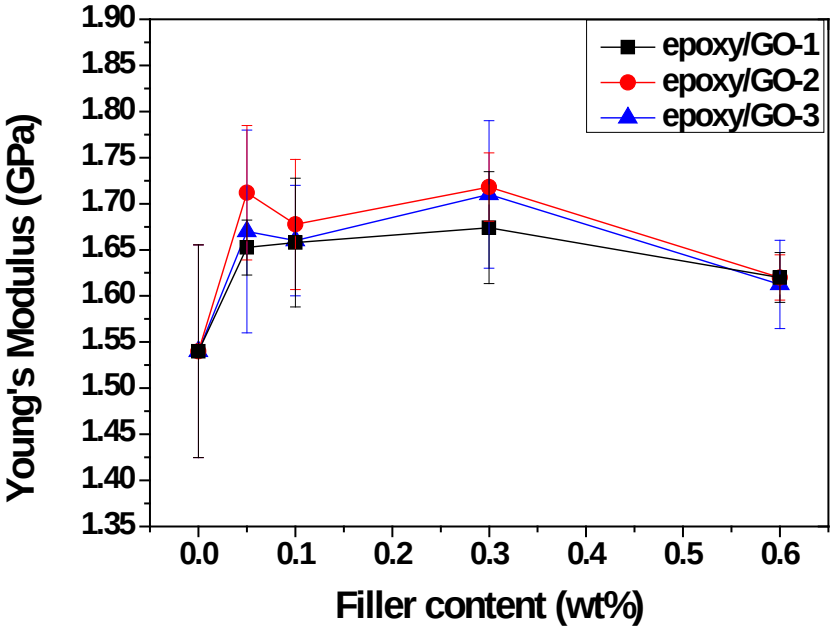

Fig. 13 - Young's modulus of epoxy and its nanocomposites with GO-3. The error bars represent standard deviations.

Fig. 14 shows DSC heat flow against temperature for the epoxy and its nanocomposites. The results indicate that the graphene sheets did not affect the curing process. The swelling result is shown in Fig. 15. The weight gain of epoxy from swelling was reduced with the addition of GO-3. It proved the role of the enhanced interfacial adhesion, which accorded with the Tg results. The thermal degradation was further measured, and the curves are drawn in Fig. 16. It was found that the incorporation of 0.1 wt% GO-3 showed a smaller mass loss of 5% in between 425 ^{o}C and 520 ^{o}C, compared with the pure epoxy. Incorporation of 0.1 wt% GO-3 resulted in an increase in the thermal stability of the epoxy. The electric conductivity of epoxy/GO-3 nanocomposites was also tested for the nanocomposites. The conductivity of the nanocomposites was less than 10^{-7} S·m^{-1}. It is clear the nanocomposites were almost electric insulated.

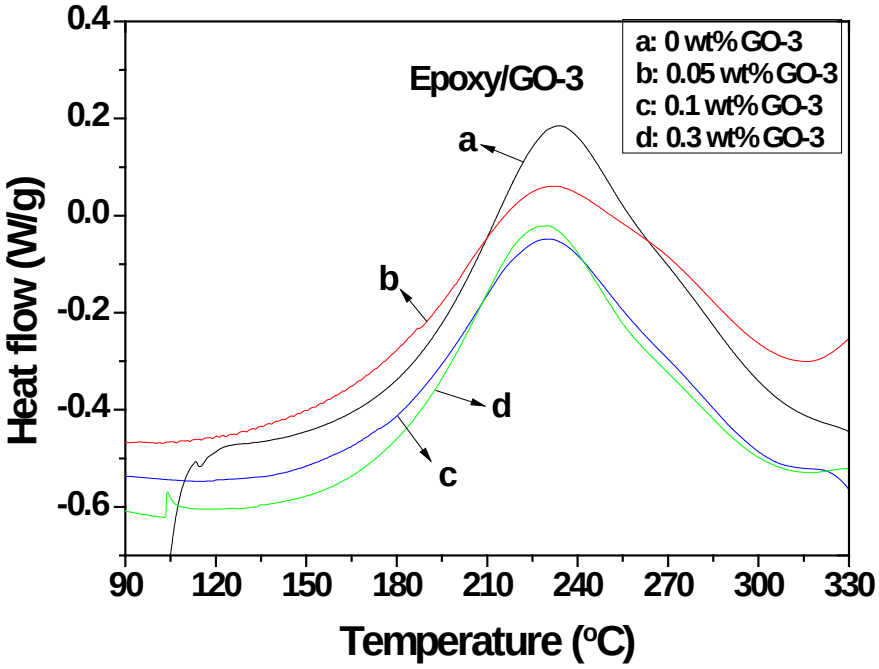

Fig. 14 - Non-isothermal DSC plots of heat flow versus temperature for epoxy/GO-3 nanocomposites.

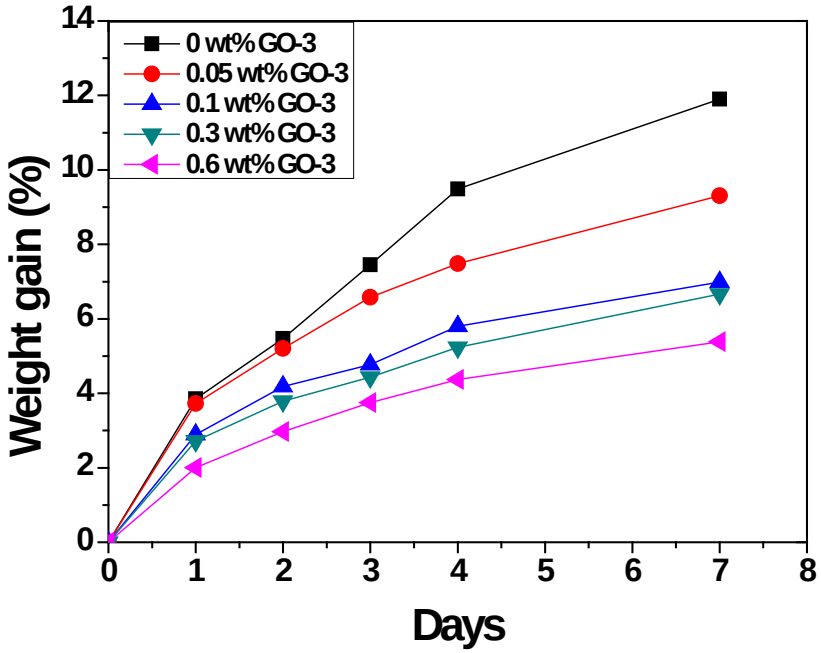

Fig. 15 – Swelling of epoxy and its nanocomposites with GO-3 in DMF at 25°C.

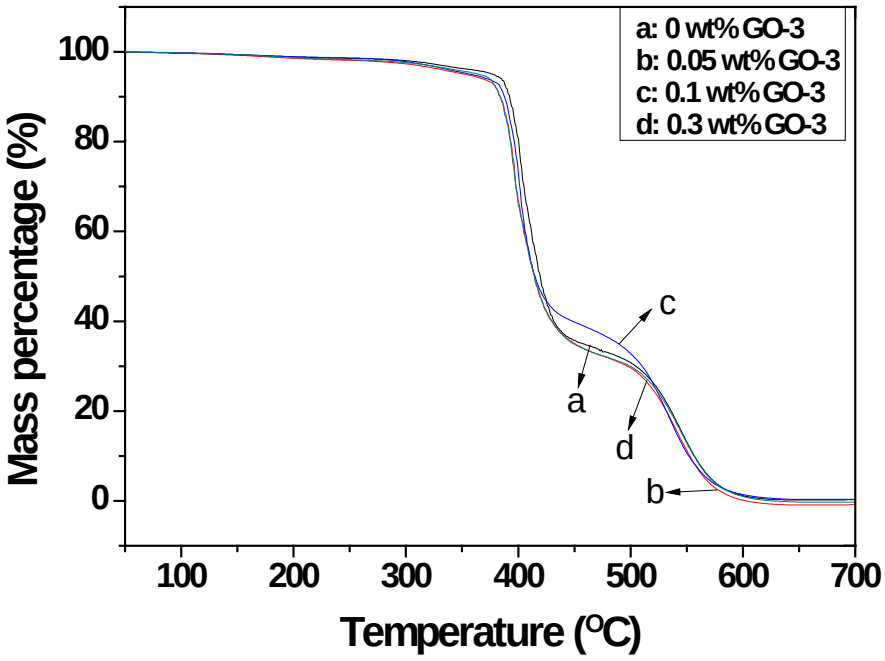

Fig. 16 - TGA degradation curves for epoxy and its nanocomposites with GO-3.

4. Conclusion

Incorporation of a very small amount of the graphene sheets into the epoxy matrix resulted in a significant improvement on the fracture toughness of the polymer. The enhancement of the epoxy toughness was strongly dependent on the size of the graphene sheets incorporated. The GO-3 with smaller sheet size (about 0.7 μm) gave a better reinforcement effect on toughness. The K_{Ic} value of the pure epoxy is about 1.32 MPa·$m^{1/2}$ and incorporation of only 0.05 wt% GO-2 or 0.1 wt% GO-3 led to a significant increase to 2.14 or 2.31 MPa·$m^{1/2}$, respectively. Based upon observation and analysis of the fracture surfaces the GO, toughening mechanism for the epoxy was well understood. The graphene sheets incorporated into the epoxy matrix more effectively disturbed to the development of crack growth and prevented crack propagation. The incorporation of GO also improved the stiffness and thermal stability of the epoxy.

REFERENCES

[1] Debdatta R. Handbook of thermoset resins. Shropshire: iSmithers; 2009.

[2] Wu SJ, Mi FL. Cure kinetics of a cyanate ester blended with poly (phenylene oxide).

Polym Int 2006;55:1296-303.

[3] Lin SC, Pearce EM. High-performance Thermosets: Chemistry, Properties, Applications. Munich, Vienna, New York: Hanser Publishers; 1993.

[4] Wetzel B, Rosso P, Haupert F, Friedrich K. Epoxy nanocomposites – fracture and toughening mechanisms. Eng Fract Mech 2006;73:2375-98.

[5] Blackman BRK, Kinloch AJ, Lee JS, Taylor AC, Agarwal R, Schueneman G, et al. The fracture and fatigue behaviour of nano-modified epoxy polymers. J Mater Sci 2007;42:7049-51.

[6] Ma J, Mo MS, Du XS, Rosso P, Friedrich K, Kuan HC. Effect of inorganic nanoparticles on mechanical property, fracture toughness and toughening mechanism of two epoxy systems. Polymer 2008;49:3510-23.

[7] Fu J, Shi L, Chen Y, Yuan S, Wu J, Liang X, et al. Epoxy nanocomposites containing mercaptopropyl polyhedral oligomeric silsesquioxane: morphology, thermal properties, and toughening mechanism. Appl Polym Sci 2008;109:340-9.

[8] Liu T, Tjiu WC, Tong Y, He C, Goh SS, Chung TS. Morphology and fracture behavior of intercalated epoxy/clay nanocomposites. J Appl Polym Sci 2004;94:1236-44.

[9] Gojny FH, Wichmann MHG, Fiedler BK, Schulte K. Influence of different carbon nanotubes on the mechanical properties of epoxy matrix composites – A comparative study. Comp Sci Technol 2005;65:2300-13.

[10] Zhang XH, Zhang ZH, Xu WJ, Chen FC, Deng JR, Deng XJ. Toughening of cycloaliphatic epoxy resin by multiwalled carbon nanotubes. Appl Polym Sci 2008;110:1351-7.

[11] Rafiee MA, Rafiee J, Wang Z, Song H, Yu Z, Koratkar N. Enhanced mechanical properties of nanocomposites at low graphene content. ACS Nano 2009;3:3884-90.

[12] Rafiee MA, Rafiee J, Srivastava I, Wang Z, Song H, Yu Z, et al. Fracture and fatigue in graphene nanocomposites. Small 2010;6:179-83.

[13] Qiu J, Wang S. Enhancing polymer performance through graphene sheets. J Appl Polym Sci 2011;119:3670-4.

[14] Palmeri MJ, Putz KW, Brinson LC. Toughening of high-performance epoxies via nanofiber sacrificial bond mechanisms. ACS Nano 2010;4:4256-64.

[15] Fang M, Zhang Z, Li J, Zhang H, Lu H, Yang Y, Constructing hierarchically structured interphases for strong and tough epoxy nanocomposites by amine-rich graphene surfaces. J Mater Chem 2010;20:9635-43.

[16] Kim H, Abdala AA, Macosko CW. Graphene/polymer nanocomposites. Macromolecules 2010;43:6515-30.

[17] Steurer P, Wissert R, Thomann R, Muelhaupt R. Functionalized graphenes and thermoplastic nanocomposites based upon expanded graphite oxide. Macromol Rapid Commun 2009;30:316-27.

[18] Prud'homme RK, Ozbas B, Aksay IA, Register RA, Adamson DH. Functional graphene – rubber nanocomposites. US Patent 7745528, 2010.

[19] Ramanathan T, Abdala AA, Stankovich S, Dikin DA, Herrera-Alonso M, Piner RD, et al. Functionalized graphene sheets for polymer nanocomposites. Nature Nanotechnol 2008;3:327-31.

[20] Faber KT, Evans AG. Crack deflection processes-I. theory. Acta Metall Mat

1983;31:565-76.

[21] Zhao Q, Hoa SV. Toughening mechanism of epoxy resins with micro/nano particles. J Compos Mater 2007;41:201-19.

[22] Chatterjee S, Nafezarefi F, Tai NH, Schlagenhauf L, Nuesch FA, Chu BTT. Size and synergy of nanofiller bybrids including graphene nanoplatelets and carbon nanotubes in mechanical properties of epoxy composites. Carbon 2012;50:5380-6.

[23] Hummers WS, Offeman RE. Preparation of graphitic oxide. J Am Chem Sco 1958;80:1339-44.

[24] Lin Y, Jin J, Song M. Preparation and characterisation of covalent polymer functionalized graphene oxide. J Mater Chem 2011;21:3455-61.

[25] Zerda AS, Lesser JA. Intercalated clay nanocomposites: morphology, mechanics, and fracture behavior. J Polym Sci Pol Phys 2001;39:1137-46.

[26] Zhu W, Low T, Perebeinos V, Bol AA, Zhu Y, Yan H, et al. Structure and electronic transport in graphene wrinkles. Nano Lett 2012;12:3431-6.

[27] Lee H, Yong HD, Kim KB, Seo Y, Yun H, Lee SW. Mechanical properties of rippled structure in suspended stacks of graphene. J Appl Phys 2010;108:014302.

[28] Wang Z, Devel M. Periodic ripples in suspended graphene. Phys Rev B 2011;83:125422.

[29] Schniepp H, Kudin KN, Li JL, Prud'homme RK, Car R, Saville DA, et al. Bending properties of single functionalized graphene sheets probed by atomic force microscopy. ACS Nano 2008;2(12):2577-84.

[30] Birley AW, Haworth B, Batchelor J. Physics of plastics: processing, properties and materials engineering. Munich, Vienna, New York, Barcelona: Hanser Publishers; 1992,

p. 342-5.

[31] Zaman I, Phan TT, Kuan HC, Meng Q, La LTB, Luong L, et al. Epoxy/graphene platelets nanocomposites with two levels of interface strength. Polymer 2011;52:1603-11.